

## Particle-hole symmetry breaking and the $\nu=5/2$ fractional quantum Hall effect

Hao Wang,<sup>1</sup> D. N. Sheng,<sup>1</sup> and F. D. M. Haldane<sup>2</sup>

<sup>1</sup>*Department of Physics and Astronomy, California State University, Northridge, California 91330, USA*

<sup>2</sup>*Department of Physics, Princeton University, Princeton, New Jersey 08544, USA*

(Received 5 December 2009; published 23 December 2009)

We report on the study of the fractional quantum Hall effect at the filling factor  $5/2$  using exact diagonalization method with torus geometry. The particle-hole symmetry breaking effect is considered using an additional three-body interaction. Both Pfaffian and anti-Pfaffian states can be the ground state depending on the sign of the three-body interaction. The results of the low-energy spectrum, the wave function overlap, and the particle-hole parity evolution, have shown clear evidence of a direct sharp transition (possibly first order) from the Pfaffian to the anti-Pfaffian state at the Coulomb point. A quantum phase diagram is established, where one finds further transitions from the Pfaffian or anti-Pfaffian state to the nearby compressible phases induced by a change of the pseudopotential.

DOI: [10.1103/PhysRevB.80.241311](https://doi.org/10.1103/PhysRevB.80.241311)

PACS number(s): 73.43.-f, 73.22.Gk, 71.10.Pm

The fractional quantum Hall effect (FQHE) at the filling factor  $\nu=5/2$  has recently drawn intensive attention in theoretical and experimental studies.<sup>1-14</sup> The Moore-Read Pfaffian (Pf) state has been proposed as a successful candidate to describe the  $5/2$  FQHE.<sup>3-5</sup> The Pf state as a non-Abelian topological phase suggests a potential application toward quantum computing.<sup>10</sup> However, the Pf state breaks particle-hole (PH) symmetry and its PH conjugate state, known as the anti-Pfaffian (APf) state, has been suggested to be another candidate state.<sup>11,12</sup> In the limit of vanishing Landau-level (LL) mixing, the Pf and APf model wave functions have the same energy for the  $5/2$  FQHE system with the pure Coulomb interaction as the system has the PH symmetry. Numerically the ground state (GS) of such a system appears as a superposition of the Pf and APf states.<sup>5,6</sup> However, the PH symmetry of the Hamiltonian in real systems can be broken by LL mixing.<sup>11-13</sup> This raises a new challenge regarding the nature of the GS realized in the experimental system,<sup>1,2</sup> which can be the Pf, APf, or superposition of them. To address this issue, we add a PH nonsymmetric three-body (3b) interaction together with the Coulomb interaction as the model Hamiltonian to reexamine the nature of the GS and to study the quantum phase transitions (QPTs) between distinct quantum phases.

In this Rapid Communication, we investigate the low-energy states of the  $5/2$  FQHE system using Lanczos method for finite-size systems with up to  $N_e=14$  electrons. The GS of a Coulomb system is found to have a transition into the Pf or APf state with the turn on of the 3b interaction. The Pf and APf states are robust in a range of the 3b interaction, insensitive to the detailed form of the 3b interaction as long as the PH symmetry is broken. The calculations on the GS wave function overlap, energy, and PH parity evolutions show the strong evidence that the phase transition between the Pf and the APf state appears to be first order, occurring exactly at the Coulomb point. Under an extra short-range pseudopotential,<sup>5</sup> Pf and APf states can have transition to the stripe phase or composite fermion liquid (CFL) phase.

We consider a two-dimensional electron system under a perpendicular magnetic field. Periodic boundary conditions for magnetic translational operators are imposed with a

quantized flux  $N_\phi$  through a rectangular unit cell  $\mathbf{L}_1 \times \mathbf{L}_2$ . The magnetic length  $\ell$  is taken as the unit of the length and the energy is in units of  $e^2/4\pi\epsilon\ell$ . To reduce the size of the Hilbert space, we carry out our calculation at every pseudomomentum  $\mathbf{K}=(K_1, K_2)$ ,<sup>15</sup> where  $K_1$  ( $K_2$ ) is in units of  $2\pi/L_1$  ( $2\pi/L_2$ ) and the even number of electrons is used for  $N_e$ . The magnetic field is assumed to be strong enough so that the spin degeneracy of the LLs is lifted.<sup>4,5,9</sup> One can thus project the system Hamiltonian into the topmost, half filled,  $N=1$  LL.<sup>5</sup> The projected Hamiltonian for the Coulomb interaction has the form

$$H_c = \frac{2}{N} \sum_{\phi} \sum_{i < j} \sum_{\mathbf{q}} e^{-q^2/2} e^{i\mathbf{q} \cdot (\mathbf{r}_i - \mathbf{r}_j)} \sum_{m=0}^{\infty} V_m L_m(q^2), \quad (1)$$

where  $V_m$  is the Haldane pseudopotential of the Coulomb interaction at  $N=1$  LL and  $L_m(x)$  is the Laguerre polynomial. The momentum  $\mathbf{q}$  is taken discrete values suitable for the unit cell lattice.  $\mathbf{r}_i$  is the guiding center coordinate of the  $i$ th electron.

The Pf state on torus can be obtained as the zero-energy GS of a repulsive 3b potential given by<sup>5</sup>

$$H_3 = - \sum_{i < j < k} S_{i,j,k} [\nabla_i^4 \nabla_j^2 \delta^2(\mathbf{r}_i - \mathbf{r}_j) \delta^2(\mathbf{r}_j - \mathbf{r}_k)], \quad (2)$$

where  $S_{i,j,k}$  is a symmetrizer. Besides the center-of-mass degeneracy, the Pf state appears at three particular pseudomomenta of  $(0, N_e/2)$ ,  $(N_e/2, 0)$ ,  $(N_e/2, N_e/2)$  (Ref. 14) as degenerate ground states. To study the effect of the PH symmetry breaking, we set up a model Hamiltonian with the form  $H=H_c+V_{3b} \cdot H_3$ . A recent work<sup>13</sup> has shown the effective 3b pseudopotential caused by the LL mixing can be negative. Thus, we allow the parameter  $V_{3b}$  change its sign and magnitude.

We first present the low-energy spectrum as shown in Figs. 1(a) and 1(b) for a pure Coulomb system with  $N_e=12$  electrons. The low-energy sector consists of six states from the three pseudomomenta of  $(0,6)$ ,  $(6,0)$ , and  $(6,6)$ , three local GSs of which are termed as the GS triplet, separating from the other excited states. The wave function overlaps with Pf and APf states demonstrate that these six states are

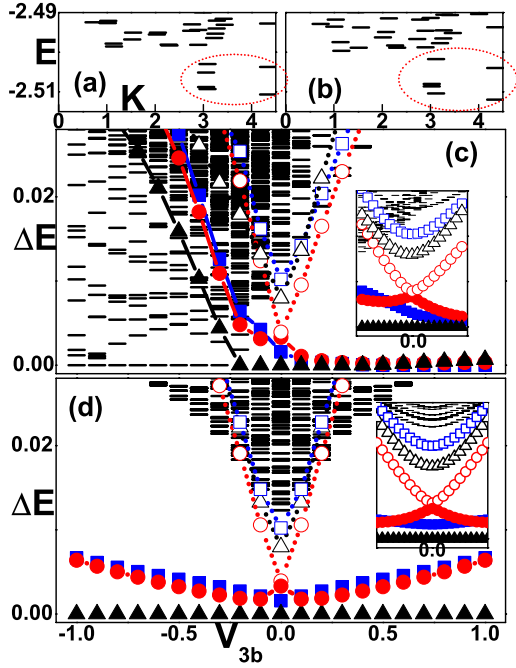


FIG. 1. (Color online) Low-lying energies as a function of the pseudomomentum  $\sqrt{K_1^2 + K_2^2}$  (in physical units) for a  $N_e=12$  pure Coulomb system with the rectangular unit cell at the aspect ratios of (a)  $L_1/L_2=0.99$ , and (b)  $L_1/L_2=0.97$ , where a pair of lowest-energy states at the pseudomomentum (0,6) are nearly degenerate. The plots of (c) and (d) are low-lying energies (relative to the globe GS) as a function of  $V_{3b}$  for the  $N_e=12$  model system with the additional 3b interaction  $H_3$  and  $H_3^*$ , respectively. The unit cell is the same as the one in (b). The circle, square and triangle symbols stand for the GSs (solid symbols) and the first excited states (open symbols) at the pseudomomenta of (0,6), (6,0), and (6,6), respectively. The insets in (c) and (d) are the zoom-in spectra for  $-0.1 < V_{3b} < 0.1$ .

closely related to the superposition states of Pf and APf. By adjusting the aspect ratio of the unit cell from  $L_1/L_2=0.99$  to 0.97 the lowest-energy pair states at the pseudomomentum (0,6) change from well separated to nearly degenerate [see also the inset of Figs. 1(c) and 1(d)]. This is consistent with the fact that the tunneling between Pf and APf in a finite-size Coulomb system is sensitive to the specific geometry of the system. The fine tuning of the aspect ratio reduces the finite-size effect by reducing the energy gap between the lowest two states at the particular pseudomomentum.

Figure 1(c) exhibits the low-lying excitation spectrum as a function of  $V_{3b}$  for the  $N_e=12$  model system with the additional 3b interaction  $H_3$ . The unit cell is the same as the one described in Fig. 1(b). At the Coulomb point ( $V_{3b}=0$ ), each GS in the GS triplet and its first excited state have the opposite PH parity. In the region of  $V_{3b} > 0$ , with  $H_3$  strength getting stronger, the degeneracy of the GS triplet improves and the energy gap between the GS triplet and other states increases. In the region of  $V_{3b} < 0$ , with the 3b strength  $|V_{3b}| < 0.1$  the near degeneracy of the GS triplet maintains. With more negative  $V_{3b}$ , the energy width of the lowest triplet increases and these energy levels cross with higher-energy states, indicating a phase transition induced by  $-H_3$ .

We further check if the obtained results depend on the

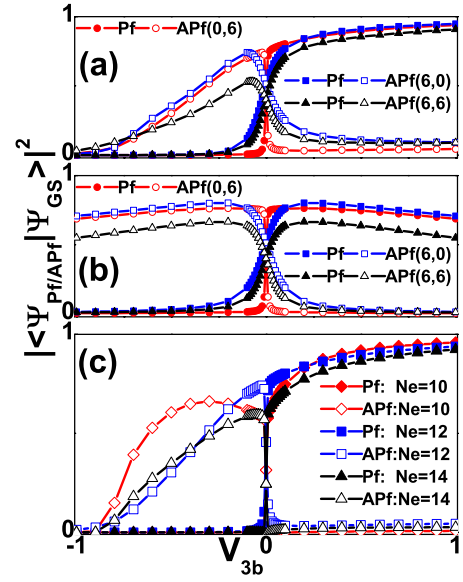


FIG. 2. (Color online) The projection of the system GS on the Pf and APf states as a function of  $V_{3b}$ . The aspect ratio  $L_1/L_2$  are 0.94, 0.97, and 0.70 for the system with  $N_e=10, 12$  and 14 electrons, respectively. The curves with solid (open) symbols stand for the projection on the Pf (APf) state. States of  $N_e=12$  system with the additional 3b interaction of (a)  $H_3$  and (b)  $H_3^*$  at pseudomomenta (0,6), (6,0), and (6,6) are represented by the curves with circle, square and triangle symbols, respectively. (c) States of  $N_e=10$  system with  $H_3$  at pseudomomentum (5,5),  $N_e=12$  at (0,6) and  $N_e=14$  at (7,7) are represented by the curves with diamond, square, and triangle symbols, respectively.

precise form of the 3b interaction. Noting that  $H_3$  has the PH symmetric and antisymmetric components, we extrapolate the PH antisymmetric component of  $H_3$ , which has the form of  $H_3^* = (H_3 - \tilde{H}_3)/2$  with  $\tilde{H}_3$  as the PH conjugate of  $H_3$ , as the other type of additional 3b interactions. This way,  $H = H_c + V_{3b} \cdot H_3^*$  has the generic form of both PH symmetric and antisymmetric parts. The obtained low-energy spectrum is shown in Fig. 1(d). Due to the PH antisymmetry of the  $H_3^*$ , the spectrum is symmetric around the Coulomb point. Clearly, the GS triplet is well separated from the excited states, indicating the establishing of Pf or APf states.

To explore the nature of the GS under the additional 3b interaction, in Fig. 2(a) we plot the wave function overlap (squared) between the GS triplet and a Pf or an APf state as a function of  $V_{3b}$  for the  $N_e=12$  model system with the 3b interaction  $H_3$  and the same unit cell as in Fig. 1(b). In the positive  $V_{3b}$  region, with the  $H_3$  strength growing, the GS projection on the Pf state monotonously increases toward unitary while the projection on the APf state decreases and drops to a small value, indicating that the GS is in the same class as the Pf state. In the negative  $V_{3b}$  region, with the strength of  $-H_3$  increasing, the projection on the Pf state quickly decreases and tends to be zero. On the other hand, the GS projection on the APf state, up to the strength  $|V_{3b}| \sim 0.1$ , increases and remains at a finite value between 0.6 and 0.7, indicating that the GS is associated with the APf in this region. When the strength increases further, the GS projection on the APf state continuously drops and eventually

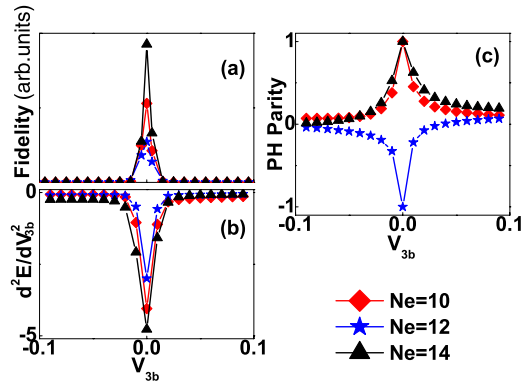


FIG. 3. (Color online) Detectors of the QPT for the model system with  $H_3$  at  $-0.1 < V_{3b} < 0.1$  and different  $N_e$ . (a) GS fidelity function, (b) second derivative of the GS energy, and (c) GS PH parity as function of  $V_{3b}$ . The curves with diamond, star, and triangle symbols represent the system with  $N_e=10, 12,$  and  $14$  electrons, respectively.

vanishes. The results for the model system with  $H_3^*$  and the same unit cell have been shown in Fig. 2(b). In the positive  $V_{3b}$  region, the projections on the APf state tend to vanish as the  $3b$  strength grows while the projections on the Pf state increase to some finite value between 0.6 and 0.7 with the strength up to 0.1, indicating the GS is associated with the Pf state. In the negative  $V_{3b}$  region, the GS has large overlap with the APf state. The above characteristics from the wave function overlaps agree with the spectrum feature shown in Figs. 1(c) and 1(d). We also notice that the projection curves of the local GS at the pseudomomentum  $(0,6)$ , which has the nearly degenerate first excited state, exhibit the sharpest transition in a small region of  $V_{3b}$  crossing the Coulomb point, indicating the strongest QPT signal. In the following discussion we target such particular GS from the GS triplet to investigate the phase transition between the Pf and the APf state. In Fig. 2(c), the results of the wave function overlap for different sizes of the system with the additional  $3b$  interaction  $H_3$  have been demonstrated. For all systems considered, the Pf state dominates on the  $V_{3b} > 0$  side while the APf states dominates on the  $V_{3b} < 0$  side as long as the  $3b$  interaction strength is smaller than 0.1 and a sharp transition occurs at the Coulomb point.

The low-lying energy spectrum and the GS wave function projections provide us with a convincing picture for the existence of a QPT toward two different states, the Pf and APf states, with the turn on of the additional  $3b$  interaction. To gain the further understanding for this QPT, we study several physical quantities for a model system near the Coulomb point. In Fig. 3 we show the evolutions of the fidelity function,<sup>16</sup> energy and PH parity of the chosen GS for different system sizes when the strength of the  $3b$  interaction  $H_3$  varies in the range  $|V_{3b}| < 0.1$  with the increment  $\delta V = 0.01$ . The pseudomenta of the chosen GSs and the unit cells for  $N_e = 10, 12, 14$  systems are the same as those in Fig. 2(c). The GS fidelity function, which we use in the plot of Fig. 3(a) to probe the response of the wave function to the variation of the parameter  $V_{3b}$ , has the form of  $F(V_{3b}) = -\frac{\text{Ln}[|\langle \Psi(V_{3b}-\delta V) | \Psi(V_{3b}+\delta V) \rangle|^2]}{\delta V^2}$ . The GS wave function is found

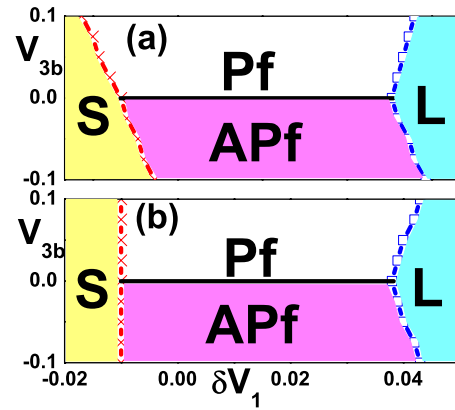


FIG. 4. (Color online) Phase diagram of  $N_e=12$  system near the Coulomb point with the  $3b$  interactions of (a)  $H_3$  and (b)  $H_3^*$ . The letters of S, L, Pf, and APf mark the phase regions of  $(\delta V_1, V_{3b})$  with the striplike, composite-fermion-liquid-like, Pf and APf phase, respectively.

insensitive to the change of the  $3b$  interaction when its strength is larger than 0.02. However, within the strength range  $|V_{3b}| < 0.02$ , the value of the fidelity function abruptly increases, indicating a QPT occurs. The peak around  $V_{3b}=0$  becomes sharper if we improve the degeneracy between the chosen GS and its first excited state by carefully tuning the parameters of the unit cell. With the sharp peak located at  $V_{3b}=0$  for all different system sizes, we can identify the Coulomb point as the transition critical point. We can also trace the GS energy to probe a QPT. In Fig. 3(b) we plot the second derivative of the GS energy as a function of  $V_{3b}$ . For all the system sizes considered, the curves exhibit the singularitylike behavior at the Coulomb point, signaling a first-order QPT. Another useful protocol for us to understand the QPT crossing  $V_{3b}=0$  is the PH parity of the GS as shown in Fig. 3(c). Within a narrow range of  $|V_{3b}| < 0.03$ , the PH parity of the GS quickly collapses from the Coulomb point, where it is either unitary or antiunitary, confirming the relation between the QPT and the PH symmetry breaking.

In a generic system with the finite LL mixing, one would expect some effective interaction terms breaking the PH symmetry, which are now modeled by  $H_3^*$ . One would also expect some effective terms with the PH symmetry, which may be modeled as a change of the Haldane pseudopotential.<sup>5</sup> We map out the quantum phase diagram for the  $5/2$  FQHE system in the presence of the  $3b$  interaction and an extra short-range pseudopotential  $\delta V_1$ . Figures 4(a) and 4(b) show the phase diagram of the  $N_e=12$  model system with the  $3b$  interaction  $H_3$  and  $H_3^*$ , respectively. We only consider the  $3b$  interaction with the strength smaller than 0.1. In this region, the GS energy changes from the Coulomb system by less than 0.5 percent and the obtained phase is most relevant for a Coulomb system with the weak PH symmetry breaking. Similar to the story in a pure Coulomb system,<sup>5</sup> we find that the model system with the weak additional  $3b$  interaction will transfer from the Pf-like or APf-like state to the compressible stripe phase when we reduce the pseudopotential  $\delta V_1$  and to the CFL phase when we increase  $\delta V_1$ . Between these two compressible phases, the Pf phase is found associated with the positive  $V_{3b}$  and the APf phase with the nega-

tive  $V_{3b}$ . For the boundary between the stripe and the Pf/APf phase, at each  $V_{3b}$  the boundary point  $\delta V_1^S$  locates where the peak value of the structure factor as a function of  $\delta V_1$  drops most dramatically. For the boundary between the Pf (APf) and CFL phases, at each  $V_{3b}$  with a positive (negative) sign, the boundary point  $\delta V_1^L$  locates where the GS projection on the CFL state begins to exceed the one on the Pf (APf) state with the square unit cell considered. As shown in Fig. 4(a), on the  $\delta V_1 > 0$  side both the Pf and the APf phase tend to expand their phase boundaries with the CFL phase when the 3b interaction strength grows. On the  $\delta V_1 < 0$  side, the Pf phase extends its boundary with the stripe phase while the APf phase shrinks. The nonsymmetric behaviors of the Pf and APf phase result from the PH symmetric component of  $H_3$ . The phase diagram of the system with 3b interaction  $H_3^*$ ,

as shown in Fig. 4(b), is symmetric around the phase line  $V_{3b}=0$ .

In summary, the PH nonsymmetric 3b term modeling a realistic 5/2 FQHE system can bring either the Pf or the APf state as the ground state depending on its sign. The pure Coulomb system is at the critical point for a possible first-order transition between these two states as one changes the sign of the 3b interaction. Our results suggest that the APf state is indeed a valid candidate<sup>11,12</sup> for the experimentally observed 5/2 FQHE.

This work is supported by U.S. NSF Grants No. DMR-0611562 and No. DMR-0906816, DOE Grant No. DE-FG02-06ER46305 (H.W. and D.N.S.), and NSF MRSEC program (Grant No. DMR-0819860) (F.D.M.H.). We also thank the KITP for support through NSF Grant No. PHY05-51164.

<sup>1</sup>R. Willett, J. P. Eisenstein, H. L. Stormer, D. C. Tsui, A. C. Gossard, and J. H. English, Phys. Rev. Lett. **59**, 1776 (1987); W. Pan, J. S. Xia, V. Shvarts, D. E. Adams, H. L. Stormer, D. C. Tsui, L. N. Pfeiffer, K. W. Baldwin, and K. W. West, *ibid.* **83**, 3530 (1999); J. S. Xia, W. Pan, C. L. Vicente, E. D. Adams, N. S. Sullivan, H. L. Stormer, D. C. Tsui, L. N. Pfeiffer, K. W. Baldwin, and K. W. West, *ibid.* **93**, 176809 (2004); J. P. Eisenstein, K. B. Cooper, L. N. Pfeiffer, and K. W. West, *ibid.* **88**, 076801 (2002).

<sup>2</sup>I. P. Radu *et al.*, Science **320**, 899 (2008).

<sup>3</sup>G. Moore and N. Read, Nucl. Phys. B **360**, 362 (1991).

<sup>4</sup>R. H. Morf, Phys. Rev. Lett. **80**, 1505 (1998).

<sup>5</sup>E. H. Rezayi and F. D. M. Haldane, Phys. Rev. Lett. **84**, 4685 (2000).

<sup>6</sup>M. R. Peterson, K. Park, and S. Das Sarma, Phys. Rev. Lett. **101**, 156803 (2008).

<sup>7</sup>M. Greiter, X. G. Wen, and F. Wilczek, Phys. Rev. Lett. **66**, 3205 (1991).

<sup>8</sup>X. Wan, Z.-X. Hu, E. H. Rezayi, and Kun Yang, Phys. Rev. B **77**, 165316 (2008).

<sup>9</sup>A. E. Feiguin, E. Rezayi, Kun Yang, C. Nayak, and S. Das Sarma, Phys. Rev. B **79**, 115322 (2009).

<sup>10</sup>S. Das Sarma, M. Freedman, and C. Nayak, Phys. Rev. Lett. **94**, 166802 (2005).

<sup>11</sup>M. Levin, B. I. Halperin, and B. Rosenow, Phys. Rev. Lett. **99**, 236806 (2007).

<sup>12</sup>S.-S. Lee, S. Ryu, C. Nayak, and M. P. A. Fisher, Phys. Rev. Lett. **99**, 236807 (2007).

<sup>13</sup>W. Bishara and C. Nayak, Phys. Rev. B **80**, 121302(R) (2009).

<sup>14</sup>M. R. Peterson, Th. Jolicoeur, and S. Das Sarma, Phys. Rev. Lett. **101**, 016807 (2008).

<sup>15</sup>F. D. M. Haldane, E. H. Rezayi, and K. Yang, Phys. Rev. Lett. **85**, 5396 (2000).

<sup>16</sup>A. Hamma, W. Zhang, S. Haas, and D. A. Lidar, Phys. Rev. B **77**, 155111 (2008).